Validation of the Flood Simulation Utilizing Satellite Observation in Japan

By Kosuke YAMAMOTO,[1)] Masato OHKI,[1)] and Kei YOSHIMURA[2), 1)]

[1)]*Earth Observation Research Center, JAXA, Tsukuba, Japan*
[2)]*Institute of Industrial Science, The University of Tokyo, Tokyo, Japan*

(Received January 11st, 2021)

This research aims to encourage feedback from observation to hydrological simulation, and to improve flood estimation. First we created an observation-based boundary condition dataset and incorporated it into the simulation to achieve higher accuracy. In addition, a comparison framework between flooded areas estimated from ALOS-2 satellite and those estimated by TE-Japan was developed. The results show that the new boundary condition data contributed to more accurate flooded area estimation, albeit to a limited extent.

Key Words: flood, ALOS-2, hydrological simulation, Today's Earth

Nomenclature

$FLDFRC$	:	flooded area fraction
G	:	target lat/lon grid
Subscripts		
TE	:	TE-Japan estimates
ALOS-2	:	ALOS-2 observation
obs_flood	:	ALOS-2 observed grid that judged as flooded
obs	:	ALOS-2 observed grid

1. Introduction

As global warming progresses, the frequency of extreme precipitation in Japan is expected to increase further, which in turn will increase the risk of floods. In reality, many people lose their lives every year due to floods caused by huge typhoons and short duration torrential rains.

In order to mitigate the damage caused by floods, it is important to predict in advance when, where, and on what scale they will occur through simulations, and to conduct on-site observations and provide information promptly after they occur. Japan Aerospace Exploration Agency (JAXA) have developed global terrestrial hydrological simulation system named Today's Earth (TE) under the joint research with The University of Tokyo[1)]. The regional version of the TE, Today's Earth – Japan (TE-Japan), enables us to see the land surface state (e.g. soil moisture, river discharge, flooded area fraction, etc.) of Japan a day or more in advance by adopting meso-scale numerical weather prediction dataset provided by Japan Meteorological Agency (JMA) as an atmospheric forcing. Forecasting accuracy has been validated by the several case studies[2)]. TE-Japan product contributes to the pre-selection of observation sites for the Advanced Land Observing Satellite-2 (ALOS-2) carrying an L-band synthetic aperture radar (SAR), and to the high accuracy and speed of flooded area estimation[3)].

In addition to the aforementioned one-way contribution from simulation to observation, this research aims to encourage feedback from observation to simulation, and to improve flood estimation by running both observation and simulation as two wheels. Specifically, we first created an observation-based boundary condition dataset and incorporated it into the simulation to achieve higher accuracy. In addition, in order to verify the effectiveness of the improvements, a comparison framework between flooded areas estimated from ALOS-2 satellite and those estimated by TE-Japan was developed.

2. Data and Methods

2.1. Overview of the TE-Japan

Fig. 1. describes the overview of the TE-Japan system. It consists of land surface model MATSIRO[5)] (Minimal Advanced Treatments of Surface Interaction and Runoff) and river routing model CaMa-Flood[6)] (Catchment-based Macro-scale Floodplain).

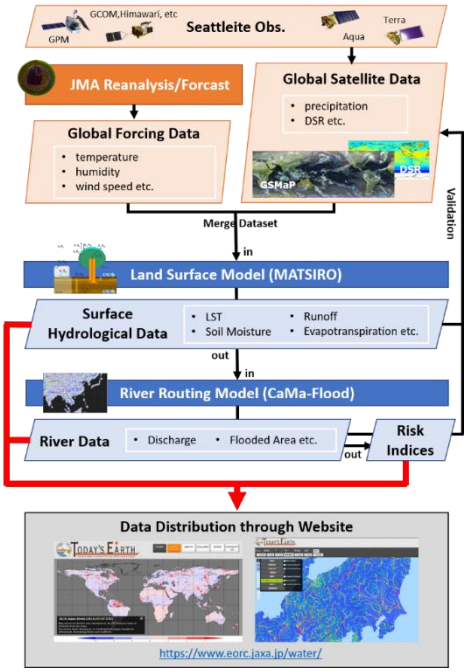

Fig. 1. Schematic flowchart of TE-Japan system.

By giving forcing of surface meteorological parameters by JMA's Numerical Weather Prediction - Meso-Scale Model (MSM), MATSIRO simulates the water and energy interactions between a land surface with a vegetation canopy and atmosphere. The surface runoff and baseflow were calculated independently using Horton flow and the advanced application in TOPMODEL[7], respectively.

Based on the calculated runoff amount, CaMa-Flood enables hydrodynamic simulation with floodplain. The model solves the local inertial equation[8], considering a rectangular river channel and trapezium flood plain storage, and represents flood plain dynamics assuming that the elevation profile of the floodplain monotonically increases in each pixel.

As of January 2022, TE-Japan is currently releasing two simulation results: MSM ver. using only MSM as input, and SAT ver. using observation data from Himawari-8 geostationary satellite for solar radiation. In this study, only the MSM ver. is used for validation.

2.2. Construction of the new boundary condition

In TE-Japan, several boundary condition data are given as external parameters. Among them, land cover data and soil data are pointed out to be in need of improvement for accurate simulation. In this study, High-Resolution Land Use and Land Cover Map Products (HRLULC)[8], a satellite-based dataset, was used to improve the former, and SoilGrids[9], a field observation-based dataset, was used to improve the latter.

HRLULC (Version 18.03) classified land cover in to 12 types with 30m grid based on the classification algorism developed in ALOS/AVNIR-2 High Resolution Land Use Land Cover map. In this study, we matched those with the land cover defined in the TE-Japan system as shown in the Table 1. Similarly, soil type data was also re-classified based on soil properties as defined by the Ministry of Agriculture, Forestry and Fisheries using SoilGrids data as shown in Table 2.

Fig. 2. and 3. are shows the example of the improvement of the re-classification. Both re-classified boundary condition datasets are reasonably express the state of the land surface compared to the original one.

Table 1. Land Cover Classification Based on HRLULC.

TE-Japan Land Cover	HRLULC (Version 18.03)
0: sea surface	-
1: continental ice	-
2: broadleaf evergreen forest	#8: EBF
3: broadleaf deciduous forest & woodland	#6: DBF
4: mixed coniferous & broadleaf deciduous forest & wood land	#20: (#6: DBF>30% + #7: DNF>30%) >90%
5: coniferous forest & woodland	#9: ENF
6: high latitude deciduous forest & woodland	#7: DNF
7: woodland c4 grassland	#5: Grassland
8: shrub & bare ground	#10: Bare land
9: tundra	-
10: cultivation	#2: Urban and built-up #3: Rice paddy #4: Crops
11: desert	-

Table 2. Soil Type Classification based on the Ministry of Agriculture, Forestry and Fisheries.

TE-Japan Soil Type	SoilGrids (Version 2.0)		
	Clay [%]	Silt [%]	Sand [%]
0: Sea Surface	0	0	0
1: Sand	0-5	0-15	85-100
2: Loamy Sand	0-15	0-15	85-95
3: Sandy Loam	0-15	0-15	65-85
4: Loam	0-15	20-45	40-65
5: Silt Loam	0-15	45-100	0-55
7: Sandy Clay Loam	15-25	0-20	5-85
8: Clay Loam	15-25	20-45	30-65
9: Silty Clay Loam	15-25	45-85	0-40
10: Sandy Clay	25-45	0-20	55-75
11: Silty Clay	25-45	45-75	0-30
12: Heavy Clay	If none of the above applied		

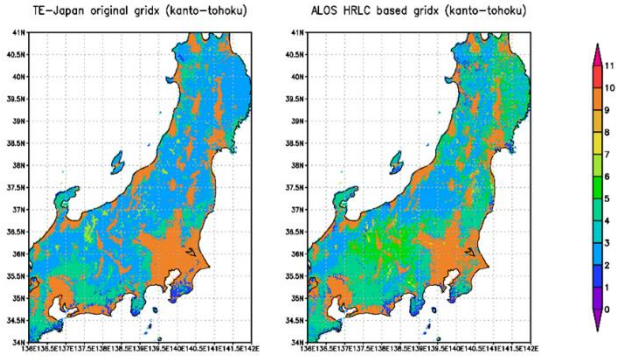

Fig. 2. TE-Japan land cover data before (left) and after (right) reclassification. The numbers in the figures are the same as those listed in Table 1.

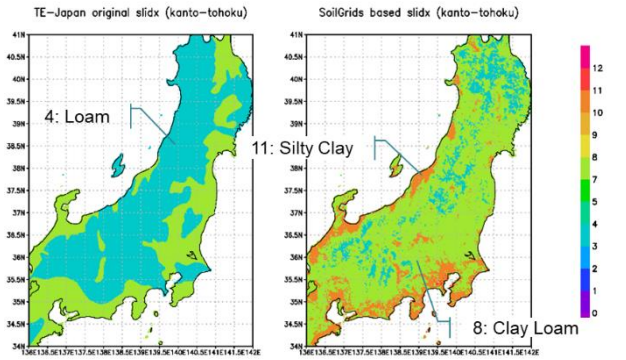

Fig. 3. TE-Japan land soil type data before (left) and after (right) reclassification. The numbers in the figures are the same as those listed in Table 2.

2.3. Development of validation framework of flooded area

In order to verify the effectiveness of the improvements, a validation framework between flooded areas estimated from ALOS-2 satellite and those estimated by TE-Japan was developed, and spatial correlation was calculated for notable flood cases. All cases that examined in this study are summarized in Table 3.

Table 1. Notable flood event over Japan (2015-2020).

Place Name	Time Stamp of the ALOS-2 Observation (JST)
Joso	11 Sep. 2015 22:56
	12 Sep. 2015 12:23
	13 Sep. 2015 23:37
	14 Sep. 2015 11:28
	16 Sep. 2015 12:20
Kitami	22 Aug. 2016 23:12
Mabi	8 Jul. 2018 00:05
Saga	28 Aug. 2019 00:18
	28 Aug. 2019 12:11
Chikuma	13 Oct. 2019 11:56
Naka	14 Oct. 2019 12:17
Chiba	26 Oct. 2019 11:36
Fukuoka	7 Jul. 2020 23:07
Kumamoto	4 Jul. 2020 13:13
	5 Jul. 2020 00:04
	6 Jul. 2020 12:18

In TE-Japan system, flooded areas are estimated in terms of the flooded area fraction ($FLDFRC_{TE}$) within the 1 min. lat/lon degree grid, whereas ALOS-2 estimates flooded areas as data enclosed by polygons. In order to directly compare these, we first convert the flooded areas estimated by ALOS-2 from polygon data to binary data of flooded/non-flooded grids with 1 sec. lat/lon resolution. Then, by calculating the fraction of flooded grids that exist in the TE-Japan 1 min. lat/lon degree grid, we get following ALOS-2 derived flooded area fraction as

$$FLDFRC_{ALOS-2} = \frac{\sum G_{obs\_flood}}{\sum G_{obs}} \quad (1)$$

where G_{obs} is the 1 sec. lat/lon grids that ALOS-2 observed, G_{obs_flood} is the grid that judged as flooded among those. Using $FLDFRC_{ALOS-2}$, spatial correlation of TE-Japan estimates was calculated.

3. Results

In Fig. 4., we pick up the case of the 2020 flood in Kyushu among the floods summarized in Table 3. The scatter plot shows that the spatial correlation of (MSM+BND) is better than that of the original TE-Japan (MSM), albeit slightly. This can be attributed to improvements in vegetation and soil type classification, which contributed to a more realistic representation of runoff processes. The same trend was observed in many of the flood cases, although not all of them will be presented here.

5. Conclusion

In this study, we reconstructed the boundary condition data for use in the TE-Japan system, and developed a framework for comparison and verification with ALOS-2 flood observations. As a result, it was found that the new boundary condition data contributed to more accurate flooded area estimation, albeit to a limited extent. In the future, we would like to improve the system's input parameters, such as precipitation and other external parameters.

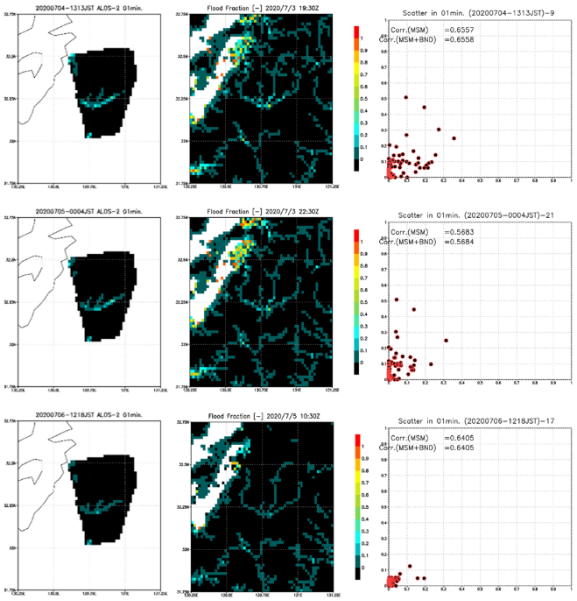

Fig. 4. Flood fraction estimated by ALOS-2(left column) and TE-Japan MSM+BND (center column). Scatter plot shows the correlation between those. Black dots shows the original TE-Japan (MSM ver.) and red circle shows the MSM+BND ver. Note that since TE-Japan does not explicitly deal with the effects of levees, dams, etc., and peaks are obtained earlier than actual floods, scatter plots are drawn for the time of highest spatial correlation within 24 hours prior to observation.

References

1) Yoshimura, K., Okazawa,T., Kim, H., Seto, S., Koiwa, Y., Oki, T., Kanae, S.: Development and Verification of a Predicting System of River Discharge over Japan JMA-MSM-GPV, *Journal of Japan Society of Civil Engineers, Ser. B1 (Hydraulic Engineering)*, **51** (2007), pp.403-408.
2) Ma, W., Ishitsuka, Y., Takeshima, A. et al. Applicability of a nationwide flood forecasting system for Typhoon Hagibis 2019. *Sci Rep* **11**, 10213 (2021). https://doi.org/10.1038/s41598-021-89522-8
3) Ohki, M.; Yamamoto, K., Tadono, T.; Yoshimura, K. Automated Processing for Flood Area Detection Using ALOS-2 and Hydrodynamic Simulation Data. *Remote Sens.* 2020, **12**, 2709. https://doi.org/10.3390/rs12172709
4) Takata, K., Emori, S., Watanabe, T., Development of the minimal advanced treatments of surface interaction and runoff, *Global and Planetary Change*, 2003, **38**, Issues 1–2, pp. 209-222.
5) Yamazaki, D., Kanae, S., Kim, H., Oki, T., A physically based description of floodplain inundation dynamics in a global river routing model, *Water Resources Research*, 2011, **47**. pp.1-21.
6) Beven, K.J., M.J. Kirkby, N. Schofield, A.F. Tagg, Testing a physically-based flood forecasting model (TOPMODEL) for three U.K. catchments, *J. Hydrol,*, 1984, **69**, Issues 1–4, pp.119-143.
7) Bates, P.D., M.S. Horritt, and T.J. Fewtrell, A simple inertial formulation of the shallow water equations for efficient two‐dimensional flood inundation modelling, *J. Hydrol.*, 2010, **387**, pp.33‐45.
8) High-Resolution Land Use and Land Cover Map Products, https://www.eorc.jaxa.jp/ALOS/en/dataset/lulc_e.htm (accessed January 10, 2022).
9) SoilGrids — global gridded soil information https://www.isric.org/explore/soilgrids (accessed January 10, 2022).